(Received 3 November 2025, Accepted 16 December 2025, Scheduled 28 February 2026)

Modified Inverted F-Shaped Microstrip Patch Antenna with Circular and Rectangular Slots and Partial Ground for the Internet of Things (IoT) Applications

Md. Arifuzzaman[1,*] and Md. Masud Rana[2]

[1] *Department of Electrical and Electronic Engineering, Varendra University, Rajshahi 6204, Bangladesh*
[2] *Department of Electrical & Electronic Engineering, Rajshahi University of Engineering and Technology, Rajshahi 6204, Bangladesh*

ABSTRACT: This paper presents an inverted F-shaped antenna with $40 \times 25 \times 1.6\,\text{mm}^3$ dimensions designed for IoT applications. It can operate in the 2.45 GHz ISM (Industrial, Scientific, and Medical) band. This antenna was constructed on an FR-4 substrate, making it well-suited for wireless applications. The antenna consisted of a reverse F-shaped radiating structure with rectangular and circular slots to obtain enhanced bandwidth and suitable return loss. The proposed antenna achieved a simulated reflection coefficient of -19.17 dB at 2.45 GHz, with a bandwidth of 23.26%. It also showed an acceptable radiation efficiency of 83.84% and a maximum gain of 3.40 dB. This provided a bidirectional pattern of radiation, which proves its quality in IoT applications. The antenna exhibited a slight difference between the simulation and measurement results, verifying its effectiveness. Moreover, the designed antenna is implemented in a home automation system to verify its validity in IoT application, and the results are highly significant.

1. INTRODUCTION

In the era of the Internet of Things (IoT), many applications are recognized across various sectors such as agriculture, security, urban development, medical body area network, and home automation. Compact, efficient, and cost-effective antennas have recently had a huge impact because of their immense opportunity to utilize many recurrences and multi-capabilities in IoT operations [1]. As a result, the demand for these structures is increasing day by day. Traditional antenna designs are considered unsuitable for wireless applications because of their stiffness and lack of flexibility. These structures must achieve a high level of conformability, be very economical and easy to design, as it is crucial in this regard [2–4]. In recent years, researchers have focused on microstrip patch antennas for IoT devices because they are lightweight, simple in design, compact, easily fabricated, suitable for frequency tuning, and compatible with planar circuits [5]. To achieve these characteristics, numerous substrate materials, including textiles, jeans, denim, polyethylene terephthalate (PET), glass, and cotton have been tested on microstrip patch antennas. Many recent works have used some of these substrates for traditional operating frequencies, such as 2.45 GHz [6]. These studies have discussed various structures of the single-band and multi-band operating antennas, such as H-shape [7], circular-shape [8], U-shaped open stub [9], M-shaped open stub [10], L-shape with coupled branch strip [11], D-shape [12], U-shape with rectangular patch inside [13], and slots in the ground plane of the antenna [14–16]. A square-shaped microstrip patch loaded with four identical slot cuts was analyzed in [17] for non-reduced dual-mode filter applications. Typical microstrip antenna designs have a narrow bandwidth, which is generally 1–2%. However, it can be improved by enhancing the thickness of the substrate and reducing the dielectric constant of the substrate [18–20]. Other techniques are also mentioned, for example, slotted antennas [21, 22], log-periodic array [23], E-shaped patches [24], and defected ground methods [25, 26]. In [27], a circular disk monopole antenna was presented to achieve a high-impedance bandwidth. New features of antennas, such as elliptical, circular, and rectangular disk monopole ones, were also offered. The elliptical antenna showed the best results. The slot technique was used in a $(70 \times 70 \times 2)\,\text{mm}^3$ antenna for multiple resonant frequencies in wearable applications [28]. In [29], a planar multiple-input multiple-output (MIMO) antenna with the capability to operate for different recommended communication bands in IoT applications was discussed. It had an overall size of $120 \times 65 \times 1.56\,\text{mm}^3$, and its main purpose was to be used for handheld devices. Another MIMO antenna was proposed in [30], which operated at four different frequencies and performed well in IoT devices. It covered (GSM, WLAN, WiMAX, and 5G) bands with an overall dimension of $60 \times 60 \times 1.6\,\text{mm}^3$. The slot technique can improve the performance of the antenna in IoT sensors [31]. For example, a dual-port antenna consisting of a slotted square patch dual-band antenna of $(38.5 \times 38.5 \times 1.6)\,\text{mm}^3$ was implemented in IoT-based industrial automation systems [32]. It had a bandwidth of 20 MHz for each resonance region. A moderately sized antenna

* Corresponding author: Md. Arifuzzaman (arifuzzaman@vu.edu.bd).

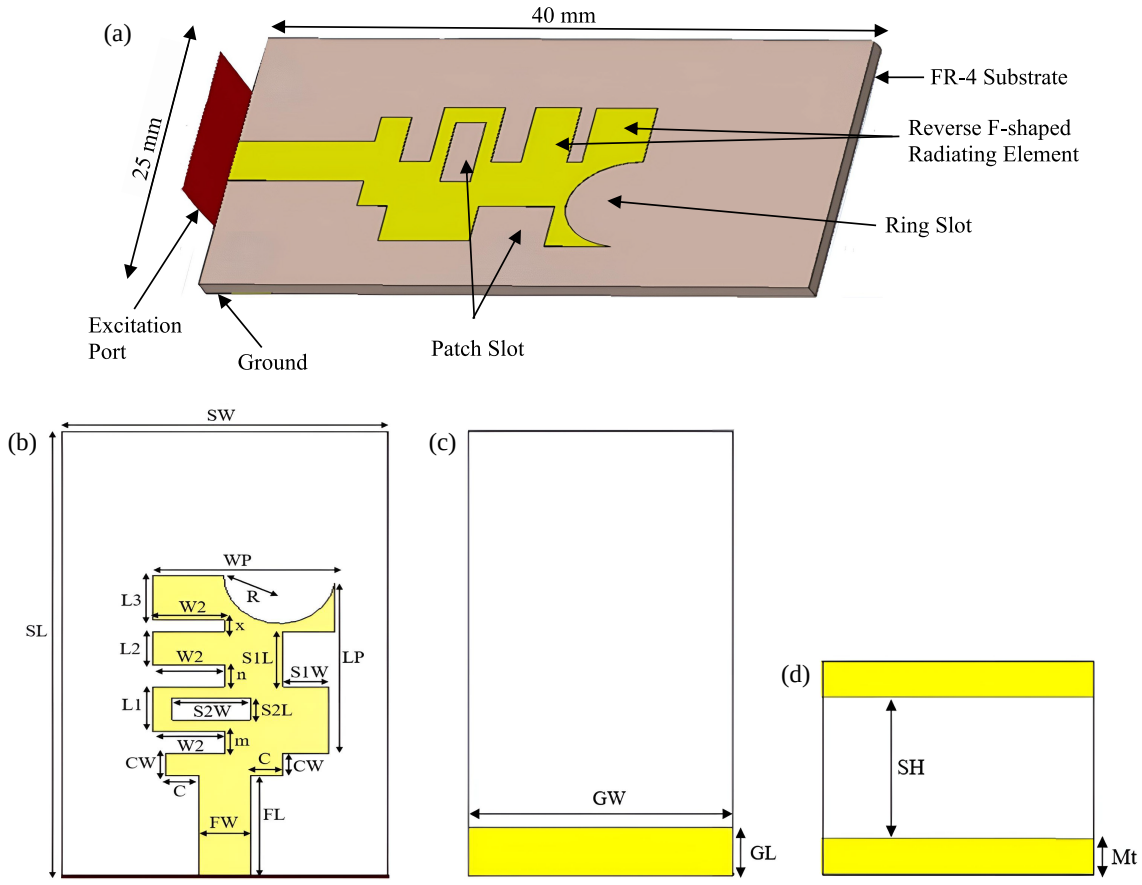

FIGURE 1. Proposed antenna geometry. (a) 3D view, (b) front view, (c) back view, and (d) side view.

incorporated square-shaped slots to enhance its quality in 5G applications [33]. A 0,127 mm thick Rogers RT5880 was selected as the substrate and showed a comparatively lower gain of approximately 4 dB at 28 GHz. In [34], a unique reconfigurable antenna was discussed, which featured an open slot and no more ground part at the rear of a mobile phone. It had a large gap of 6 mm in the metal rim and provided better reconfigurable and miniaturized results with the help of varactor diodes. The geometry of the antenna was optimized to get a higher gain and compact size in the paper [35]. Arrays can also play an important role in improving the peak gain of an antenna without degrading other parameters [36–38]. In [39], a direct-fed antenna for a smartphone with a solid metal rim was proposed. The slots were separated into two portions. To do this, two grounded points were inserted, which created a dual-loop antenna, and it showed a good radiation pattern. Fractal-based structures have been applied to reduce antenna size. 2.4 GHz antennas based on the Hilbert-fractal created small antennas for IoT devices with a size of $7 \times 3 \times 2\,\text{mm}^3$ [40].

This paper presents an antenna with compact size, good bandwidth, and impedance matching by using a modified inverted F-shaped radiating element with rectangular and circular slots. An undefected partial ground has also been implemented to have an enhanced bandwidth and a smaller reflection coefficient. This structure achieves an improved bandwidth of 23.26% and a moderately reduced return loss of −19.17 dB. It also exhibits a radiation efficiency of 83.84% which is higher than the standard value for any antenna.

2. ANTENNA DESIGN METHODOLOGY

2.1. Geometry of the Proposed Antenna

The structure of the proposed antenna is shown in Figure 1(a). The antenna has compact dimensions of $40 \times 25 \times 1.6\,\text{mm}^3$ with the help of an inverted F-shaped patch element, and rectangular and circular slot cuts. These features provide a wider bandwidth with accurate impedance matching. An undefected partial ground has been used in this antenna in order to increase the bandwidth and return loss. The conventional feed line method has been used to connect the antenna elements. The antenna works in the ISM band of 2.45 GHz when the feed line is subjected to excitation. An FR-4 lossy material of thickness 1.6 mm, relative permittivity ε_r of 4.4, and loss tangent of 0.025 is the substrate for this antenna.

Furthermore, to determine the influence of the structural parameters on the performance of the proposed antenna, a parametric analysis was performed.

Figure 1(b) presents the design of the front part of the proposed antenna. Figure 1(c) shows the back part of the antenna, which consists of a partial ground without any slot. Figure 1(d) shows the side view of the antenna with the height of both the

TABLE 1. Optimized parameters of the proposed antenna.

Parameter	Size (mm)	Parameter	Size (mm)	Parameter	Size (mm)
SL	40	*FL*	9	*R*	4.3
SW	25	*FW*	4	*GL*	5
LP	15.3	*C*	2.5	*GW*	25
WP	14	*CW*	2	*SH*	1.6
L1	4	*S1L*	5	*Mt*	0.035
L2	3	*S1W*	3.4	m	2
L3	4	*S2L*	2	n	2
W2	5.5	*S2W*	6	x	1

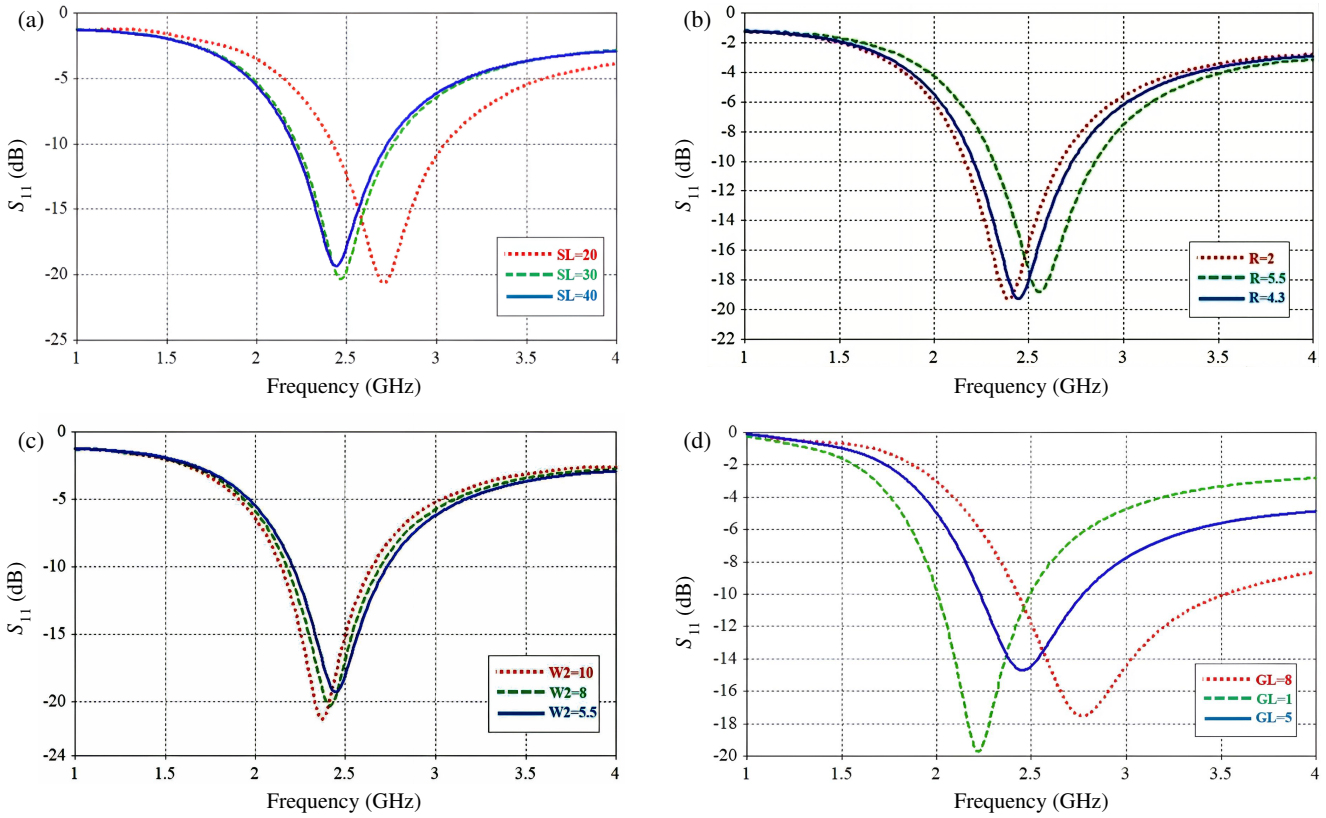

FIGURE 2. The effects of (a) substrate length (SL), (b) ring slot radius (R), (c) patch width ($W2$), and (d) ground length (GL) on the reflection coefficient of the proposed antenna.

substrate and patch. The updated parameters of the mentioned antenna are listed in Table 1.

2.2. Parametric Analysis

In this section, the effects of some parameters on the resonant frequency, bandwidth, efficiency, gain, and impedance matching properties are explained using a precise parametric analysis. The length of the substrate, radius of the circular slot, width of the patch element, and height of the ground are the factors that influence the parameters of the mentioned antenna. Figure 2(a) illustrates the reflection coefficient (S_{11}) from the Computer Simulation Technology (CST) simulation for the different substrate lengths (SL). It is noticeable that a decreased SL value causes the right shifting of the S_{11} from the resonant frequency of 2.45 GHz, but an increase in SL causes the opposite. However, an upgraded value of S_{11} and a wide bandwidth at a 2.45 GHz frequency can be obtained when the value of SL is 40 mm. The results of varying the ring slot radius (R) on the return loss are shown in Figure 2(b). When the radius of the slot cut is more than 4.3 mm, the graph of the return loss shifts to the right of the resonance frequency. The opposite scenario occurs when the value is less than 4.3 mm. For the value of $R = 4.3$ mm, the perfect bandwidth and S_{11} are achieved. Figure 2(c) shows the effects of patch width ($W2$) on S_{11}.

For a patch width of 10 mm, the reflection coefficient curve resonates at 2.34 GHz. However, as it needs to be resonated at 2.45 GHz, the value of the patch width is kept changing until the perfect result is reached. Finally, for a patch width of

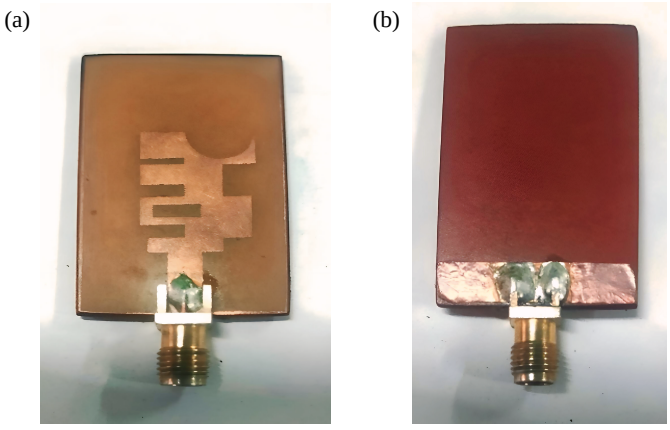

FIGURE 3. (a) Front and (b) back view of the fabricated antenna.

5.5 mm, better bandwidth and impedance matching are secured. The variation in ground length (GL) has also been tested on S_{11} which is depicted in Figure 2(d). The significantly lower value of GL means the left shift of the S_{11} curve from 2.45 GHz. If the value increases to more than 5 mm, the curve resonates at more than 2.45 GHz. The figure reveals that 5 mm is the perfect ground height for this design.

From the parametric sweep, it can be summarized that a reduced return loss and better impedance matching are obtained for $SL = 40$ mm, $R = 4.3$ mm, $W2 = 5.5$ mm, and $GL = 5$ mm. As a result, these parameters have been chosen as the optimized parameters.

3. RESULTS AND DISCUSSION

3.1. Numerical and Experimental Results

Initially, the simulation of the proposed antenna model has been performed using the optimized parameters listed in Table 1. The CST simulation software has been used to complete this task. After that, the antenna has been fabricated. Then, with the help of a Vector Network Analyzer (VNA), the S_{11} and voltage standing wave ratio (VSWR) have been calculated in the open space. Since pure FR-4 material is unavailable, glass fiber has been selected as the substrate material. Figures 3(a) and (b) show the fabricated images of the proposed antenna. The necessary experimental setup for measuring the parameters of the fabricated antenna is shown in Figure 4.

FIGURE 4. Setup for measurement.

3.1.1. Return Loss (S_{11} Parameter) and VSWR

Figure 5 illustrates a comparison between the results of the return loss and VSWR with respect to the frequency obtained from the measurement and simulation. From the simulation, the achieved S_{11} of the proposed antenna is -19.17 dB at 2.45 GHz resonant frequency with a bandwidth of 570 MHz (2.19–2.76 GHz), that is, 23.26% bandwidth. The value of the VSWR is 1.24, which means that it can provide very good impedance matching.

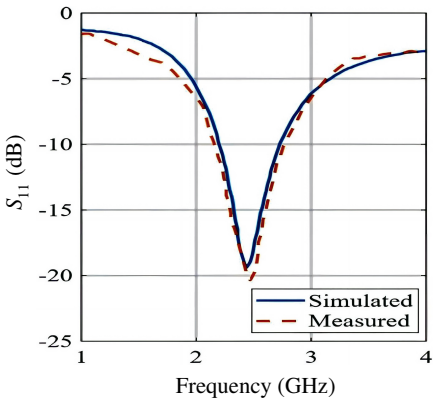

FIGURE 5. Simulated and measured S_{11}.

From the measurements, the proposed antenna shows a S_{11} of -20.35 dB at 2.45 GHz, including a band of 2.16–2.76 GHz (600 MHz) or 24.48% in percentage. Moreover, the measured VSWR value is 1.15. Therefore, there is a slight difference between simulated and measured results.

Several manufacturing defects, such as imprecise fabrication and impurities of FR-4 material may have occurred. There are also some problems with the instruments.

3.1.2. Radiation Pattern

The radiation behavior of the described antenna is given in Figure 6. This antenna provides a main lobe and a side lobe of 2.34 dB and -0.8 dB, respectively, at 2.45 GHz. The main lobe exhibits a direction of 168° at the resonance frequency. Because it possesses both main and side lobes, it can function as a bi-directional antenna. However, the simulated results could not be verified by experimental data because of the inaccessibility of the anechoic chamber.

3.1.3. Gain

The realized gain of the proposed antenna achieved from the simulation is shown in Figure 7. It has a maximum gain of 3.40 dB at 2.45 GHz, which is considered a standard value for traditional antennas using an FR-4 substrate.

3.1.4. Efficiency

Figure 8 illustrates the efficiency of the radiation of the discussed antenna. It is evaluated as a percentage in this study and has a value of 83.84% at a resonant frequency of 2.45 GHz which exceeds the standard value of efficiency for any antenna.

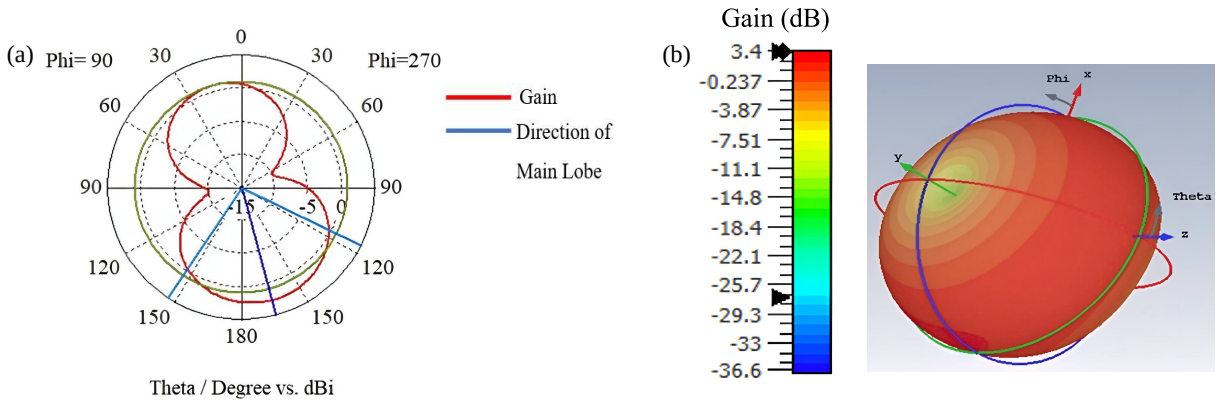

FIGURE 6. Radiation pattern of the antenna at 2.45 GHz in (a) 1D form and (b) 3D form.

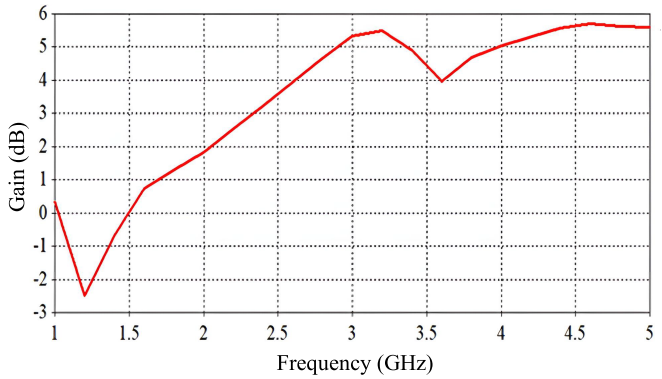

FIGURE 7. Realized gain of the proposed antenna.

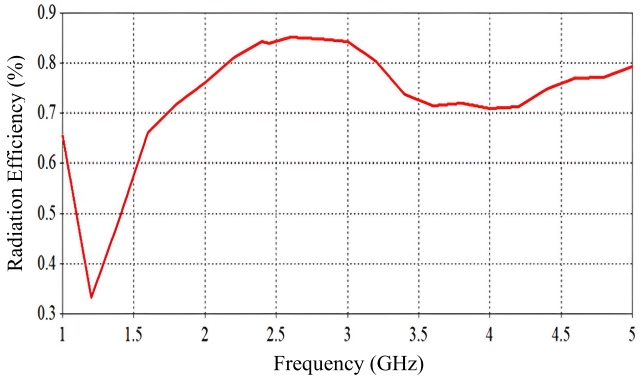

FIGURE 8. Radiation efficiency of the proposed antenna.

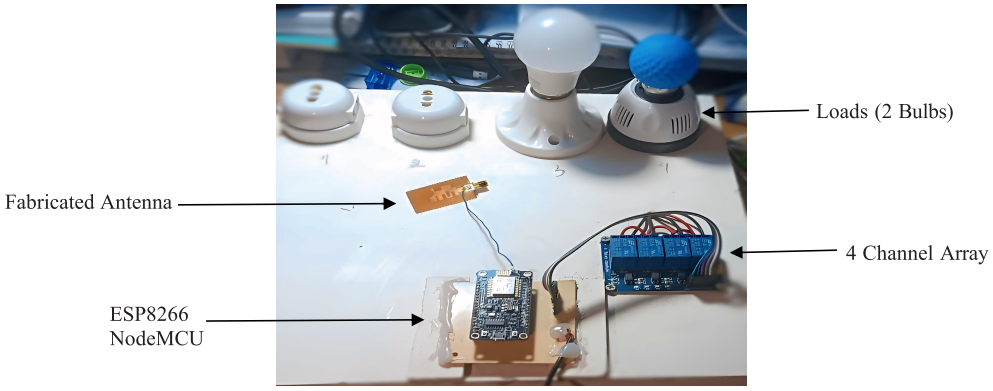

FIGURE 9. Experimental setup for IoT-based home automation system incorporating proposed antenna.

3.2. Implementation of the Proposed Antenna in IoT-Based Home Automation System

It is necessary to apply the antenna to any IoT-related system to demonstrate its capability in IoT applications. Therefore, after finishing the fabrication process, the fabricated antenna is connected to a home automation system based on the IoT, which is depicted in Figure 9. At first, the inherent antenna in the ESP8266 NodeMCU was scratched in some places, and then, the fabricated antenna was patched onto those places of ESP8266 NodeMCU. Thus, the proposed antenna cancels the influence of the built-in antenna in ESP8266 and takes its role itself. As the fabricated antenna operates properly in the IoT-based home automation system, it can be said that it inherits the capacity to perform in any type of IoT based system.

4. COMPARISON WITH THE EXISTING ANTENNAS

An inverted-F-shaped microstrip patch antenna with rectangular and circular slots for upgrading bandwidth, gain, and impedance matching is presented in this paper. A partial ground technique has also been implemented in this structure to improve the gain and return loss. Previous studies discussed different design methods, such as meander line, L-shaped, S-shaped, monopole, MIMO, cage structures, and circular slots, which show their benefits.

TABLE 2. Comparative analysis of the proposed antenna model with the existing antenna models.

Ref.	Size (mm^2)	Antenna Type	Resonant Frequency (GHz)	Bandwidth (%)	Gain (dB)	Application	Comparison with the Proposed Antenna
[1]	100×40	S-shaped	2.4	3.30	Not Specified	WLAN	Lower bandwidth and larger size
[41]	10×19	Uniplanar Meandered	2.4	8.00	1.20	TD-LTE/WLAN	Lower bandwidth
[42]	75.7×75.7	Circular Slotted Patch	2.4	6.53	6.58	WBAN	Lower bandwidth and larger size
[43]	49×49	Cage Antenna	2.4	3.50	3.00	WLAN	Lower bandwidth and larger size
[44]	15×90.86	Monopole Meander Line	2.4	4.00	2.00	WLAN	Lower bandwidth and larger size
[30]	30×20	Planar MIMO	1.8	4.44	1.5	IoT	Lower bandwidth and larger size
			2.4	7.91	2.5		
			3.4	13.23	2.8		
			5.4	9.25	3.6		
[45]	28×21	L-shaped	2.4	5.83	2.09	IoT	Lower bandwidth and larger size
[46]	40×10	Meander Line with Defected Ground and Parasitic Patch	2.4	8.75	1.14	IoT	Low gain with low bandwidth
This Work	**40×25**	**Inverted F-shaped with Circular and Rectangular Slot**	**2.45**	**23.26**	**3.40**	**IoT**	**Small size with high bandwidth**

Table 2 illustrates a comparison between the proposed antenna design and the antenna structures described in previous studies. From the comparative analysis shown in Table 2, the proposed antenna has higher bandwidths than the other existing antennas. Again, it has a higher gain than all of them except the antenna in [42]. Moreover, the design discussed in this paper features an inverted-F shape, partial ground, a circular slot, and two rectangular slots, which have not yet been implemented in previous studies. This combination upgrades impedance matching by providing smaller return losses. This antenna is more compact than many other designs.

5. CONCLUSION

In this paper, a modified inverted-F-shaped microstrip patch antenna suitable for IoT-based systems has been developed. This suggested antenna operates at 2.45 GHz, providing a bandwidth of 570 MHz. The structure of the suggested antenna was influenced by the study in [5]. For the substrate, an FR-4 lossy material has been selected. It represents an inverted-F-shaped patch element, in which rectangular and circular slots are cut. An undefected partial ground has also been implemented on the back side of the antenna. All of these features have been used in order to gain a compact size, wider bandwidth, and better impedance matching. The overall dimensions of the antenna are $40 \times 25 \times 1.6\,mm^3$. The reflection coefficient of the antenna from the simulation is -19.17 dB at 2.45 GHz with a band of 570 MHz. It also maintains a VSWR of 1.24, which indicates perfect impedance matching. The measurement process is done with VNA, and it shows a return loss of -20.35 dB, a band of 600 MHz (24.48%), and a VSWR of 1.15. Minor dissimilarities between the simulated and measured results have occurred because of instrumental defection. The antenna also provides a radiation efficiency of 83.84% along with a gain of 3.40 dB. Finally, the proposed antenna has been tested on an IoT-based home automation system to justify its ability to function in IoT applications.

6. FUTURE WORK

- FR-4 material inherits several limitations, including poor operation at high frequency, inability in Ultra-High Frequency (UHF) applications, low thermal conductivity, and very high absorption rate of moisture. So, textile or nanocomposite materials can be used as alternative substrates to overcome these obstacles [47, 48].
- A MIMO antenna can perform well in this application. As the proposed antenna combines slots and partial ground and provides improved bandwidth and efficiency. Future arrangements could concentrate on converting it into a MIMO antenna [49].

REFERENCES

[1] Ibrahim, H. H., M. J. Singh, S. S. Al-Bawri, S. K. Ibrahim, M. T. Islam, M. S. Soliman, and M. S. Islam, "Low profile monopole meander line antenna for WLAN applications," *Sensors*, Vol. 22, No. 16, 6180, Aug. 2022.

[2] Awan, W. A., A. Abbas, S. I. Naqvi, D. H. Elkamchouchi, M. Aslam, and N. Hussain, "A conformal tri-band antenna for flexible devices and body-centric wireless communications," *Micromachines*, Vol. 14, No. 10, 1842, 2023.

[3] Sabban, A., "Wearable circular polarized antennas for health care, 5G, energy harvesting, and IoT systems," *Electronics*, Vol. 11, No. 3, 427, 2022.

[4] Sharma, M., "Design and analysis of multiband antenna for wireless communication," *Wireless Personal Communications*, Vol. 114, No. 2, 1389–1402, 2020.

[5] Ali, W., N. Nizam-Uddin, W. M. Abdulkawi, A. Masood, A. Hassan, J. A. Nasir, and M. A. Khan, "Design and analysis of a quad-band antenna for IoT and wearable RFID applications," *Electronics*, Vol. 13, No. 4, 700, 2024.

[6] Hashim, F. F., W. N. L. B. W. Mahadi, T. B. A. Latef, and M. B. Othman, "Fabric-metal barrier for low specific absorption rate and wide-band felt substrate antenna for medical and 5G applications," *Electronics*, Vol. 12, No. 12, 2754, 2023.

[7] Das, R. and H. Yoo, "A wideband circularly polarized conformal endoscopic antenna system for high-speed data transfer," *IEEE Transactions on Antennas and Propagation*, Vol. 65, No. 6, 2816–2826, Jun. 2017.

[8] Yun, S., K. Kim, and S. Nam, "Outer-wall loop antenna for ultra-wideband capsule endoscope system," *IEEE Antennas and Wireless Propagation Letters*, Vol. 9, 1135–1138, 2010.

[9] Soora, S., K. Gosalia, M. S. Humayun, and G. Lazzi, "A comparison of two and three dimensional dipole antennas for an implantable retinal prosthesis," *IEEE Transactions on Antennas and Propagation*, Vol. 56, No. 3, 622–629, Mar. 2008.

[10] Zaki, A. Z. A., E. K. I. Hamad, T. G. Abouelnaga, H. A. Elsadek, S. A. Khaleel, A. J. A. Al-Gburi, and Z. Zakaria, "Design and modeling of ultra-compact wideband implantable antenna for wireless ISM band," *Bioengineering*, Vol. 10, No. 2, 216, Feb. 2023.

[11] Shah, S. A. A. and H. Yoo, "Scalp-implantable antenna systems for intracranial pressure monitoring," *IEEE Transactions on Antennas and Propagation*, Vol. 66, No. 4, 2170–2173, Apr. 2018.

[12] Padhi, S. K., N. C. Karmakar, C. L. Law, and S. Aditya, "A dual polarized aperture coupled circular patch antenna using a C-shaped coupling slot," *IEEE Transactions on Antennas and Propagation*, Vol. 51, No. 12, 3295–3298, 2003.

[13] Liu, W.-C., C.-M. Wu, and Y. Dai, "Design of triple-frequency microstrip-fed monopole antenna using defected ground structure," *IEEE Transactions on Antennas and Propagation*, Vol. 59, No. 7, 2457–2463, Jul. 2011.

[14] Dayo, Z. A., M. Aamir, S. A. Dayo, I. A. Khoso, P. Soothar, F. Sahito, T. Zheng, Z. Hu, and Y. Guan, "A novel compact broadband and radiation efficient antenna design for medical IoT healthcare system," *Mathematical Biosciences and Engineering*, Vol. 19, No. 4, 3909–3927, 2022.

[15] Huang, Z., H. Wu, S. S. Mahmoud, and Q. Fang, "Design of a novel compact MICS band PIFA antenna for implantable biotelemetry applications," *Sensors*, Vol. 22, No. 21, 8182, 2022.

[16] Palandoken, M., "Compact bioimplantable MICS and ISM band antenna design for wireless biotelemetry applications," *Radioengineering*, Vol. 26, No. 4, 917–923, 2017.

[17] Al-Yasir, Y. I. A., M. K. Alkhafaji, H. A. Alhamadani, N. O. Parchin, I. Elfergani, A. L. Saleh, J. Rodriguez, and R. A. Abd-Alhameed, "A new and compact wide-band microstrip filter-antenna design for 2.4 GHz ISM band and 4G applications," *Electronics*, Vol. 9, No. 7, 1084, 2020.

[18] Kumar, A., N. Gupta, and P. C. Gautam, "Gain and bandwidth enhancement techniques in microstrip patch antennas — A review," *International Journal of Computer Applications*, Vol. 148, No. 7, 9–14, 2016.

[19] Elsagheer, R. M., "Study on bandwidth enhancement techniques of microstrip antenna," *Journal of Electrical Systems and Information Technology*, Vol. 3, No. 3, 527–531, 2016.

[20] Parizi, S. A. R., "Bandwidth enhancement techniques," in *Trends in Research on Microstrip Antennas*, Vol. 1, Intech Open, London, UK, 2017.

[21] Sumithra, P. and D. Kannadassan, "Bandwidth enhancement of low-profile slot antennas using theory of characteristic modes," *AEU — International Journal of Electronics and Communications*, Vol. 138, 153868, 2021.

[22] Moussa, K. H., A. S. I. Amar, M. Mabrouk, and H. G. Mohamed, "Slotted E-shaped meta-material decoupling slab for densely packed MIMO antenna arrays," *Micromachines*, Vol. 12, No. 8, 873, 2021.

[23] Mistry, K. K., P. I. Lazaridis, Z. D. Zaharis, and T. H. Loh, "Design and optimization of compact printed log-periodic dipole array antennas with extended low-frequency response," *Electronics*, Vol. 10, No. 17, 2044, 2021.

[24] Vincenti Gatti, R., R. Rossi, and M. Dionigi, "Single-layer line-fed broadband microstrip patch antenna on thin substrates," *Electronics*, Vol. 10, No. 1, 37, 2021.

[25] Wang, J., W. Cui, Y. Zhou, R. Liu, M. Wang, C. Fan, H. Zheng, and E. Li, "Design of wideband antenna array with dielectric lens and defected ground structure," *Electronics*, Vol. 10, No. 17, 2066, 2021.

[26] Peng, H., R. Zhi, Q. Yang, J. Cai, Y. Wan, and G. Liu, "Design of a MIMO antenna with high gain and enhanced isolation for WLAN applications," *Electronics*, Vol. 10, No. 14, 1659, 2021.

[27] Agrawall, N. P., G. Kumar, and K. P. Ray, "Wide-band planar monopole antennas," *IEEE Transactions on Antennas and Propagation*, Vol. 46, No. 2, 294–295, 1998.

[28] Mandal, D. and S. S. Pattnaik, "Quad-band wearable slot antenna with low SAR values for 1.8 GHz DCS, 2.4 GHz WLAN and 3.6/5.5 GHz WiMAX applications," *Progress In Electromagnetics Research B*, Vol. 81, 163–182, 2018.

[29] Jha, K. R., B. Bukhari, C. Singh, G. Mishra, and S. K. Sharma, "Compact planar multistandard MIMO antenna for IoT applications," *IEEE Transactions on Antennas and Propagation*, Vol. 66, No. 7, 3327–3336, 2018.

[30] Thiruvenkadam, S., E. Parthasarathy, S. K. Palaniswamy, S. Kumar, and L. Wang, "Design and performance analysis of a compact planar MIMO antenna for IoT applications," *Sensors*, Vol. 21, No. 23, 7909, 2021.

[31] Wang, M., L. Yang, and Y. Shi, "A dual-port microstrip rectenna for wireless energy harvest at LTE band," *AEU — International Journal of Electronics and Communications*, Vol. 126, 153451, 2020.

[32] Abdulkawi, W. M., A. F. A. Sheta, I. Elshafiey, and M. A. Alkanhal, "Design of low-profile single- and dual-band antennas for IoT applications," *Electronics*, Vol. 10, No. 22, 2766, 2021.

[33] Li, J. L., M. H. Luo, and H. Liu, "Design of a slot antenna for future 5G wireless communication systems," in *2017 Progress In Electromagnetics Research Symposium — Spring (PIERS)*, 739–741, St. Petersburg, Russia, 2017.

[34] Stanley, M., Y. Huang, H. Wang, H. Zhou, Z. Tian, and Q. Xu, "A novel reconfigurable metal rim integrated open slot antenna for octa-band smartphone applications," *IEEE Transactions on Antennas and Propagation*, Vol. 65, No. 7, 3352–3363, Jul. 2017.

[35] Dhengale, B. B. and D. C. Karia, "A 5.8 GHz ISM band microstrip antenna for RFID applications," in *2015 International Conference on Nascent Technologies in the Engineering Field (ICNTE)*, 1–4, Navi Mumbai, India, Jan. 2015.

[36] Li, K., L.-J. Xu, Z. Duan, Y. Tang, and Y. Bo, "Dual-band and dual-polarized repeater antenna for wearable applications," in *2018 IEEE MTT-S International Wireless Symposium (IWS)*, 1–3, Chengdu, China, May 2018.

[37] Wang, Q., N. Mu, L. Wang, J. Liu, and Y. Wang, "Miniaturization microstrip antenna design based on artificial electromagnetic structure," in *2017 Sixth Asia-Pacific Conference on Antennas and Propagation (APCAP)*, 1–3, Xi'an, China, Oct. 2017.

[38] Majidi, N., G. G. Yaralioglu, M. R. Sobhani, and T. Imeci, "Design of a quad element patch antenna at 5.8 GHz," in *2018 International Applied Computational Electromagnetics Society Symposium (ACES)*, 1–2, Denver, CO, USA, Mar. 2018.

[39] Ban, Y.-L., Y.-F. Qiang, Z. Chen, K. Kang, and J.-H. Guo, "A dual-loop antenna design for hepta-band WWAN/LTE metal-rimmed smartphone applications," *IEEE Transactions on Antennas and Propagation*, Vol. 63, No. 1, 48–58, Jan. 2015.

[40] Anguera, J., A. Andújar, J. Jayasinghe, V. V. S. S. S. Chakravarthy, P. S. R. Chowdary, J. L. Pijoan, T. Ali, and C. Cattani, "Fractal antennas: An historical perspective," *Fractal and Fractional*, Vol. 4, No. 1, 3, 2020.

[41] Srivastava, T., S. Saurabh, A. Vyas, and R. Mishra, "A triple band $ shape slotted PIFA for 2.4 GHz and 5 GHz WLAN applications," *Soft Computing: Theories and Applications*, 399–406, 2019.

[42] Naidu, P. V., A. Kumar, and R. Rajkumar, "Design, analysis and fabrication of compact dual band uniplanar meandered ACS fed antenna for 2.5/5 GHz applications," *Microsystem Technologies*, Vol. 25, No. 1, 97–104, 2019.

[43] El Atrash, M., O. F. Abdalgalil, I. S. Mahmoud, M. A. Abdalla, and S. R. Zahran, "Wearable high gain low SAR antenna loaded with backed all-textile EBG for WBAN applications," *IET Microwaves, Antennas & Propagation*, Vol. 14, No. 8, 791–799, Jul. 2020.

[44] Liu, Z., Y. Zhang, Y. He, and Y. Li, "A compact-size and high-efficiency cage antenna for 2.4-GHz WLAN access points," *IEEE Transactions on Antennas and Propagation*, Vol. 70, No. 12, 12 317–12 321, 2022.

[45] Zambak, M. F., S. S. Al-Bawri, M. Jusoh, A. H. Rambe, H. Vettikalladi, A. M. Albishi, and M. Himdi, "A compact 2.4 GHz L-shaped microstrip patch antenna for ISM-band Internet of Things (IoT) applications," *Electronics*, Vol. 12, No. 9, 2149, 2023.

[46] Prottoy, S. S., M. M. Rana, M. A. Islam, M. Arifuzzaman, and N. Alam, "Inverse S-shaped meander line antenna loaded with slotted parasitic patch and defected ground for Internet of Things (IoT) applications," *Progress In Electromagnetics Research C*, Vol. 154, 31–38, 2025.

[47] Al-Gburi, A. J. A., N. H. M. Radi, T. Saeidi, N. J. Mohammed, Z. Zakaria, G. S. Das, A. Buragohain, and M. M. Ismail, "Superconductive and flexible antenna based on a tri-nanocomposite of graphene nanoplatelets, silver, and copper for wearable electronic devices," *Journal of Science: Advanced Materials and Devices*, Vol. 9, No. 3, 100773, 2024.

[48] Al-Gburi, A. J. A., M. M. Ismail, N. J. Mohammed, A. Buragohain, and K. Alhassoon, "Electrical conductivity and morphological observation of hybrid filler: Silver-graphene oxide nanocomposites for wearable antenna," *Optical Materials*, Vol. 148, 114882, 2024.

[49] Pandya, K., T. Upadhyaya, U. Patel, V. Sorathiya, A. Pandya, A. J. A. Al-Gburi, and M. M. Ismail, "Performance analysis of quad-port UWB MIMO antenna system for Sub-6 GHz 5G, WLAN and X band communications," *Results in Engineering*, Vol. 22, 102318, 2024.